

## Measurement of Compound Nucleus Space-Time Extent with Two-Neutron Correlation Functions

N. Colonna,<sup>1</sup> D. R. Bowman,<sup>2</sup> L. Celano,<sup>1</sup> G. D'Erasmus,<sup>3</sup> E. M. Fiore,<sup>3</sup> L. Fiore,<sup>1</sup> A. Pantaleo,<sup>1</sup> V. Paticchio,<sup>1</sup> G. Tagliente,<sup>1</sup> and S. Pratt<sup>4</sup>

<sup>1</sup>*Istituto Nazionale Fisica Nucleare, V. Amendola 173, 70126 Bari, Italy*

<sup>2</sup>*Atomic Energy of Canada, Ltd., Chalk River Laboratories, Ontario, K0J 1J0 Canada*

<sup>3</sup>*Dipartimento di Fisica-Universita', V. Amendola 173, 70126 Bari, Italy*

<sup>4</sup>*Department of Physics and Astronomy, Wayne State University, Detroit, Michigan 48201*

(Received 10 April 1995)

Two-neutron relative-momentum correlation functions have been measured in the 130 MeV  $^{18}\text{O} + ^{26}\text{Mg}$  reaction. Differences in the longitudinal and transverse correlation functions, observed for the first time for neutrons, allow an independent determination of the spatial extent and the time scale for decay of the  $^{44}\text{Ca}$  compound nucleus. A comparison with theoretical calculations indicates a radius of  $4.4 \pm 0.3$  fm and an average neutron emission time scale of  $1100 \pm 100$  fm/c for  $^{44}\text{Ca}$  at 100 MeV excitation energy. Correlation functions selected by cuts on the total momentum of the neutron pair give a quantitative characterization of the cooling of a compound nucleus.

PACS numbers: 25.70.Gh, 25.70.Pq

The relative wave function of two identical particles is influenced by quantum-statistical interference, by the short-range nuclear interaction, and, for charged particles, by the long-range Coulomb force. The magnitude of the influence of these effects depends mainly on the space-time separation of the particles. Hence two-particle relative-momentum correlation functions can be used to probe the space-time extent of emission sources [1]. The multidimensionality of this correlation function, i.e., the dependence on the relative and total momentum vectors of the two-particle system, may be exploited to provide independent information about the spatial extensions and the lifetime of a source.

Many such studies of excited nuclear matter have been performed with probes of pions [2] or kaons [3] at relativistic and ultrarelativistic energies, and with protons [4], photons [5], or emitted nuclear fragments [2,6] at intermediate energy. However, there have been few studies of the interferometry of true compound nuclei at low excitation energy [7]. These studies are important in order to observe directly the effect of quantum-statistical interference in fermionic systems [8,9] and to test the decay widths predicted by statistical decay models [8–12].

Energetic considerations require that identical-particle correlations at low excitation energy be limited to two-proton or two-neutron pairs. The delicate interplay between the repulsive effect of quantum-statistical interference and the attractive final-state nuclear interaction is obscured in two-proton correlation functions because of the presence of the Coulomb force [13]. This makes theoretical interpretation of these correlation functions very difficult. In contrast, two-neutron correlation functions are easier to interpret theoretically, but are affected by experimental problems such as detector cross talk, in and out scattering, and low detection efficiency. For these

reasons two-neutron correlation functions have not been extensively studied [8,9,13–15].

In this paper we present two-neutron correlation functions measured in the reaction of  $^{18}\text{O} + ^{26}\text{Mg}$  at an incident energy of 130 MeV. These correlation functions are interpreted in the same manner as a wide body of two-proton measurements [4] by employing a formalism incorporating both quantum-statistical interference and final-state nuclear interactions [16].

The experiment was performed at the XTU Tandem Accelerator of the Laboratori Nazionali di Legnaro, Italy. A pulsed beam of  $^{18}\text{O}$  at 130 MeV incident energy was focused onto a  $^{26}\text{Mg}$  target of  $5 \text{ mg/cm}^2$  areal density. The typical intensity was  $\sim 8 \times 10^9$  particles/s. Neutrons were detected in a cluster of 18 close-packed detectors, which was placed at a distance of 2 m from the target and centered at  $\sim 45^\circ$ . The cluster subtended approximately  $18^\circ$  in plane and  $34^\circ$  out of plane. To allow for cross-talk rejection (described below), adjacent detectors were separated by a center-to-center distance of 20.7 cm (minimum distance of 8 cm), which corresponded to an angular separation of  $\sim 6^\circ$ . Four additional detectors were placed at angles of  $20^\circ$ ,  $80^\circ$ ,  $100^\circ$ , and  $130^\circ$ . Each neutron detector consisted of a cylindrical cell of BC501 liquid scintillator, with both a diameter and a length of 12.7 cm. In and out scattering of neutrons were minimized by mounting the detectors far from any walls at a height of  $\sim 2$  m, and by employing light aluminum supports and a thin (3 mm) aluminum scattering chamber.

The energy of the detected neutrons was determined from the time of flight (TOF) relative to the radio-frequency signal of the bunched beam. The neutron energy resolution, resulting from the time resolution of the beam (1.5 ns FWHM and of the detectors 1.2 ns FWHM) and the uncertainty in the interaction position within the

detectors, varied from 6% to 8% for energies between 3 and 25 MeV. Prompt  $\gamma$  rays were rejected by TOF and also used to calibrate the TOF spectra. A neutron- $\gamma$  ray discrimination technique was also applied to reject all environmental background. The deposited energy was calibrated with sources of  $^{60}\text{Co}$  and  $^{137}\text{Cs}$  and recorded during the experiment. A software energy threshold of a 1 MeV electron equivalent was then applied in the analysis. Coincidences between two or more detectors were used as a trigger for most of the experiment, but some data were also collected with a singles trigger, in order to measure inclusive energy and angular distributions.

The cross section for fusion in the 130 MeV  $^{18}\text{O} + ^{26}\text{Mg}$  reaction is estimated to exhaust 90% of the total reaction cross section [17]. Contamination from nonfusion reactions is discriminated against because of the lower neutron multiplicity in these reactions. Furthermore, neutrons evaporated from projectilelike fragments are virtually excluded because of unfavorable kinematical focusing, while neutrons from targetlike fragments are predominantly below threshold because of the low temperature and small laboratory velocity of the emitting source.

Neutron energy spectra, corrected for detection efficiency [18], are shown in Fig. 1 (symbols). The spectra resemble Maxwell distributions, which are typical of emission from a thermalized source. A quantitative check of the compound nucleus origin of the detected neutrons has been obtained with a single-source fit to the measured energy distributions [19,20]. The fit, shown as solid curves, reproduces quite well the measured spectra. A source velocity of  $0.0547c$  and a temperature of 2.75 MeV are obtained with the fit. These values are consistent with the compound nucleus velocity of  $0.0509c$  and its initial average thermal energy per nucleon of 1.4 MeV [21].

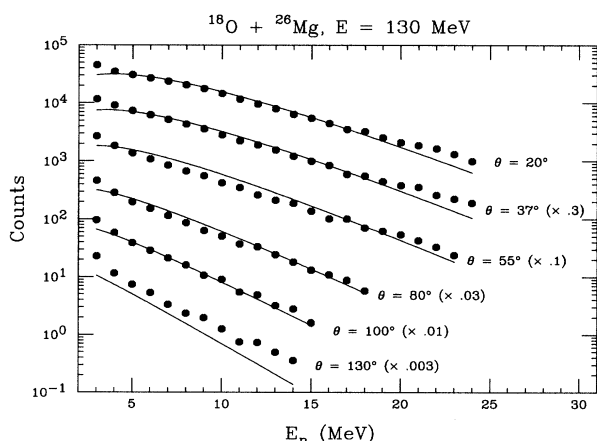


FIG. 1. Neutron energy spectra measured at the indicated laboratory angles. The curves represent the results of a single-source fit using the form of Ref. [19]. The efficiency correction on the 3 MeV point is estimated to be affected by a 40% uncertainty; above 6 MeV the estimated systematic uncertainty is less than 5%.

As mentioned above, measurements of two-neutron correlation functions are plagued by experimental difficulties, in particular by neutron in scattering and detector cross talk. Because of the small amount of material in the vicinity of the detectors, simulations indicate that in scattering was minimal in the present experimental setup. Furthermore, because of the large flight path for in-scattered neutrons, any residual contamination was suppressed by a 3 MeV threshold on neutron energy.

The scattering of a neutron from one detector into another presents a much more complex problem. If the scattered neutron leaves an appreciable signal in both detectors, the spurious coincidence may greatly distort the true two-neutron correlation function. Because of the close packing of the detectors in the cluster, and because of the low multiplicity of emitted neutrons in this reaction, it was estimated that more than 50% of the detected two-neutron coincidences were produced by neutron cross talk. In order to suppress cross talk [9], a coincidence between two detectors was attributed to cross talk, and therefore rejected if it fulfilled the following relation:

$$\frac{1}{2} m \left( \frac{d_{\min}}{\Delta t} \right)^2 < E_1, \quad (1)$$

Here  $d_{\min}$  is the minimum distance between the struck detectors,  $\Delta t$  is the time difference between the signals from the two detectors, and  $E_1$  is the energy of the first neutron. The left side of the equation represents the minimum energy a neutron scattered from the first detector would need in order to reach the second detector in the measured time interval  $\Delta t$ . To take the experimental uncertainties into account, 3 standard deviations ( $\sigma \sim 1$  ns) were added to the measured time  $\Delta t$ ,  $3\sigma$  were subtracted from the TOF of the first neutron, and  $E_1$  was calculated assuming the interaction occurred at the front face of the detector. Both simulations and tests with an  $^{241}\text{Am}/^9\text{Be}$  source indicate that the condition (1) is very effective in rejecting cross-talk neutrons, since  $< 0.3\%$  of cross-talk events survive it. Along with cross-talk neutrons a large number of true two-neutron coincidences are also rejected by (1). However, it was estimated from simulations that condition (1) reduces the residual contamination of cross talk in the correlation functions to the level of  $\sim 1\%$ .

The experimental correlation functions (see below) constitute a self-consistent check of the absence of cross-talk contamination. When the rejection condition (1) is not applied, or when less stringent conditions are applied, a peak occurs at a relative momenta of 10–15 MeV/ $c$ , resulting from the finite time difference between cross-talk neutrons. More stringent conditions, on the other hand, produce a decrease in statistics but no appreciable difference in the observed correlation functions.

The experimental correlation functions were constructed from the measured neutron coincidence ( $Y_{12}$ ) and single-particle ( $Y_i$ ) yields as

$$1 + R(q) = C \sum \frac{Y_{12}(\mathbf{p}_1\mathbf{p}_2)}{Y_1(\mathbf{p}_1)Y_2(\mathbf{p}_2)}. \quad (2)$$

For a given relative momentum  $q$ , the sum extended over all neutron energies and detector combinations. The normalization constant  $C$  was determined by the requirement that  $R = 0$  for large relative momenta ( $20 < q < 50$  MeV/c). Although the singles spectra are not affected by cross talk, condition (1) must also be applied in the denominator in order to compensate for true coincidences rejected in the numerator.

A source with a nonzero emission time scale has a phase-space distribution of emitted neutrons which is elongated in the direction parallel to the total neutron momentum. Along the short direction, perpendicular to the total neutron momentum, the fermionic anticorrelation from quantum statistics is stronger and reduces the positive correlation from the attractive final state interaction. A narrow cut on the transverse orientation shows this suppression. Transforming the neutron momenta into the frame of a well-characterized source is crucial for detecting lifetime effects [22]. A compound nucleus reaction at low incident energy represents the ideal case in this respect, since it leads to the formation of a unique source with a well-defined velocity.

In Fig. 2, longitudinal (solid symbols,  $0^\circ < \psi_s < 60^\circ$ ) and transverse (open symbols,  $80^\circ < \psi_s < 90^\circ$ ) correlation functions were generated by gating on  $\psi_s$ , the angle between the relative and the total momentum of the neutron pair,  $\psi_s = \cos^{-1}(\mathbf{q} \cdot \mathbf{P}'/qP')$ . Here the total momentum  $\mathbf{P}'$  is expressed in the compound nucleus (complete fusion) rest frame. Angle-gated correlation functions in the laboratory frame do not exhibit differences [22].

To quantify the neutron emission time scale, we have compared the measured angle-gated correlation functions with theoretical calculations obtained by convoluting an

assumed phase space distribution with the two-neutron relative wave function [2,4,16,23]. Neutrons were assumed to be emitted from a source with a characteristic emission time scale  $\tau$  and radius  $r_0$ , and with momenta sampled from the source-frame experimental distribution [see Eq. (2) of [22]]. After transforming into the laboratory frame, the cross-talk rejection procedure (1) was applied to the simulated neutron pair. To incorporate the energy and angular resolution of the apparatus, the neutron momenta were randomized over the volume of each detector prior to the convolution with the relative wave function and the results were assigned to the relative momentum bin corresponding to an interaction in the center of the detector.

Comparisons were performed for a large range of source radii and emission time scales, and a reduced  $\chi^2$  between the experimental and theoretical results was calculated for each combination of  $R$  and  $\tau$ . The  $\chi^2$  was calculated for the range of relative momenta ( $0 < q \leq 20$  MeV/c), in which a correlation was observed. The minimum value of  $\chi^2$  (see panel in Fig. 2) is obtained with a radius of  $\sim 4.4$  fm and an emission time scale of  $\sim 1100$  fm/c (or  $3.7 \times 10^{-21}$  s). In Fig. 2 the theoretical angle-gated correlation functions are shown for these values of  $R$  and  $\tau$ ; similarly good agreement is obtained for combinations of the radius and the emission time scale in the range  $R = 4.1\text{--}4.7$  and  $\tau = 1000\text{--}1200$  fm/c [24].

The measured neutron emission time scale of 1100 fm/c is, as expected, shorter than that found for the same compound nucleus at a lower excitation energy [8], and is similar to the proton emission time scale found for systems of similar mass and excitation energy [10–12].

The extracted value of 1100 fm/c should be considered only as an average neutron emission time. The instantaneous decay rate is determined by the compound nucleus decay width, which depends strongly on temperature. As a result of particle evaporation, cooling occurs, and an evolution of the emission time scale during the decay is to be expected. Since the energy of the emitted particles is also sensitive to the compound nucleus temperature, evidence for cooling can be found by analyzing correlation functions gated on the total momentum of the particle pair [4,25].

The average separation between emitted neutrons is proportional to  $(P_{c.m.}/2m_n)\tau$ , where  $P_{c.m.}$  is the neutron-pair total momentum in the source frame and  $m_n$  the neutron mass. For a momentum-independent emission time scale, the two-neutron correlation becomes more attenuated with increasing momentum, since the average neutron-neutron separation increases. In Fig. 3, the angle-integrated correlation functions are shown for two cuts on  $P_{c.m.}$  in the compound nucleus rest frame. The measured correlation functions gated on larger total momenta [Fig. 3(a)] are not attenuated, but are rather slightly stronger relative to those of smaller total momenta [Fig. 3(b)]. This observation is qualitatively consistent with a faster emission time for higher energy neutrons.

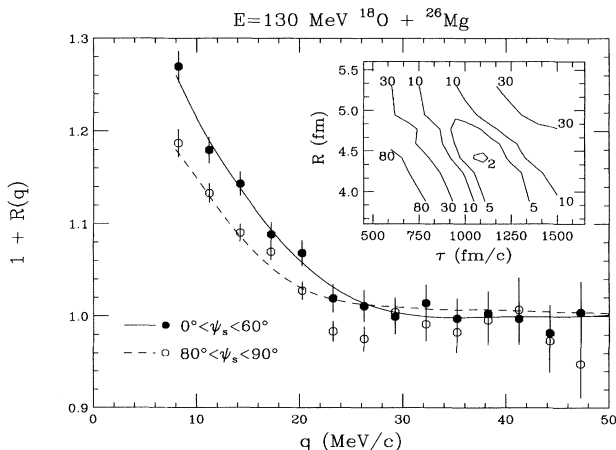


FIG. 2. Experimental longitudinal (solid symbols) and transverse (open symbols) correlation functions. The solid and dashed curves depict calculations (see text for details) with a source radius  $R = 4.4$  fm and lifetime of  $\tau = 1100$  fm/c. The panel in the figure is a contour diagram of the reduced  $\chi^2$  between the experimental and theoretical correlation functions in the region of  $q = 0\text{--}20$  MeV/c.

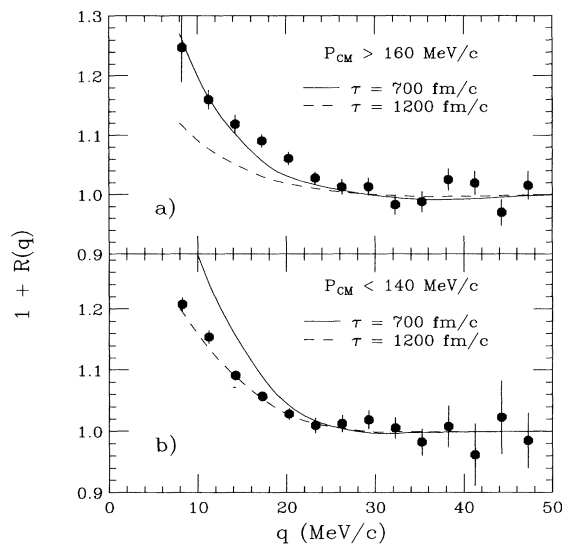


FIG. 3. Angle-integrated correlation functions for two cuts on the total neutron pair momentum in the compound nucleus frame. The solid and dashed curves are results of theoretical calculations with the indicated emission time scales.

For a quantitative estimate of the cooling effect, we have compared the momentum-gated correlation functions with the calculations described above. The radius in the calculations was fixed at a value of 4.4 fm, which gave the best agreement with the angle-gated correlation functions. The comparisons (curves in Fig. 3) indicate that the neutrons with larger total momenta are emitted on a time scale of approximately 700 fm/c. Pairs with smaller momentum are emitted on a longer time scale of approximately 1200 fm/c. As suggested by the momentum dependence of the correlation functions found with charged-particle pairs [4,25–27], this measured difference provides a quantitative characterization of the cooling of a compound nucleus.

Simulations suggest that while the cross-talk rejection procedure does not strongly affect the angle-gated correlation function, it introduces a sizeable distortion on the momentum-gated correlation functions by modifying the relative weights of longitudinal and transverse configurations. For this reason it is of fundamental importance to apply the same cross-talk rejection procedure to the simulated correlation functions and the data.

In conclusion, we have presented the first angle- and momentum-gated two-neutron correlation functions for a long-lived compound nucleus. The observed differences between the longitudinal and transverse correlation functions have been exploited to accurately determine the compound nucleus radius and the average neutron emission time scale. Angle-integrated correlation functions gated on the total pair momentum show evidence for cooling of the compound nucleus. This work demonstrates

that two-neutron correlation functions are a powerful tool for investigation the space-time characteristics of compound nuclei.

The authors wish to thank G. Antuofermo, G. Iacobelli, A. Masciullo, M. Sacchetti and P. Vasta for technical support, the operations crew and A. Facco and G. Fortuna at LNL for providing a good quality, high intensity pulsed beam. The authors gratefully acknowledge discussions with G. Viesti.

- 
- [1] R. Hanbury-Brown and R. Q. Twiss, *Nature (London)* **178**, 1046 (1956).
  - [2] D. H. Boal, C. K. Gelbke, and B. K. Jennings, *Rev. Mod. Phys.* **62**, 553 (1990), and references therein.
  - [3] H. Beker *et al.*, *Nucl. Phys.* **A566**, 115c (1994).
  - [4] W. Bauer, C. K. Gelbke, and S. Pratt, *Ann. Rev. Nucl. Part. Sci.* **42**, 77 (1992), and references therein.
  - [5] M. Marqués *et al.*, *Phys. Rev. Lett.* **73**, 34 (1994).
  - [6] C. K. Gelbke, *Nucl. Phys.* **A538**, 65c (1992).
  - [7] S. E. Koonin, W. Bauer, and A. Schäfer, *Phys. Rev. Lett.* **62**, 1247 (1989).
  - [8] W. Dünneweber *et al.*, *Phys. Rev. Lett.* **65**, 297 (1990).
  - [9] R. Gentner *et al.*, *Z. Phys. A* **343**, 401 (1992).
  - [10] P. A. DeYoung *et al.*, *Phys. Rev. C* **39**, 128 (1989).
  - [11] P. A. DeYoung *et al.*, *Phys. Rev. C* **41**, R1885 (1990).
  - [12] R. A. Kryger *et al.*, *Phys. Rev. C* **46**, 1887 (1992).
  - [13] B. Jakobsson *et al.*, *Phys. Rev. C* **44**, R1238 (1991).
  - [14] K. Ieki *et al.*, *Phys. Rev. Lett.* **70**, 730 (1993).
  - [15] P. A. DeYoung *et al.*, (to be published).
  - [16] S. Pratt and M. B. Tsang, *Phys. Rev. C* **36**, 2390 (1987).
  - [17] W. J. Swiatecki, *Nucl. Phys.* **A376**, 275 (1982); S. Bjornholm and W. J. Swiatecki, *Nucl. Phys.* **A391**, 471 (1982).
  - [18] M. Aghinolfi *et al.*, *Nucl. Instrum. Methods* **165**, 217 (1979); A. Pantaleo *et al.*, *Nucl. Instrum. Methods Phys. Res., Sect. A* **291**, 570 (1990).
  - [19] K. Yoshida *et al.*, *Phys. Rev. C* **46**, 961 (1992).
  - [20] L. Fiore *et al.*, *Phys. Rev. C* **47**, R1835 (1993).
  - [21] This value is obtained by subtracting the rotational energy from the total excitation energy. The rotational energy was calculated from angular momenta up to  $37 \hbar$  (the critical value for a vanishing fission barrier). The average thermal energy corresponds to a temperature of 3.4 MeV for a level density parameter  $a = A/8 \text{ MeV}^{-1}$ .
  - [22] M. A. Lisa *et al.*, *Phys. Rev. Lett.* **71**, 2863 (1993); M. A. Lisa *et al.*, *Phys. Rev. C* **49**, 2788 (1994).
  - [23] W. G. Gong *et al.*, *Phys. Rev. C* **43**, 1804 (1991).
  - [24] A single normalization constant calculated from the ungated correlation functions was used for both angle-gated correlation functions. The results do not change dramatically, however, if independent normalization constants are used; in this case, in fact, the minimum  $\chi^2$  is obtained from  $R = 4.2$  and  $\tau = 1050 \text{ fm/c}$ .
  - [25] W. G. Gong *et al.*, *Phys. Rev. C* **43**, 781 (1991).
  - [26] J. M. Alexander *et al.*, *Phys. Rev. C* **48**, 2874 (1993).
  - [27] A. Elmaani *et al.*, *Phys. Rev. C* **49**, 284 (1994).